Electronic Supplementary Material (ESI) for New Journal of Chemistry.

Density functional theory study of Ni_x (x=4-16) cluster impregnation effects in multi-metal (Ce, Ti) UiO-66 metal organic frameworks

Phanikumar Pentyala, Prakash Biswas, Prateek K. Jha*

Department of Chemical Engineering, Indian Institute of Technology Roorkee, Roorkee 247667, India

*Corresponding author; Email: prateek.jha@ch.iitr.ac.in

Supporting Information

Table S1: **Nomenclature of the different Ni_x impregnated configurations**

Explanation	Name of configuration
Ce/Zr-UiO-66 (16.6%)	L_{Ce}
Ni_4 in Ce/Zr-UiO-66 (16.6%)	L_{Ce}-Ni_4
Ni_8 in Ce/Zr-UiO-66 (16.6%)	L_{Ce}-Ni_8
Ni_{12} in Ce/Zr-UiO-66 (16.6%)	L_{Ce}-Ni_{12}
Ni_{16} in Ce/Zr-UiO-66 (16.6%)	L_{Ce}-Ni_{16}
Ce/Zr-UiO-66 (33.3%)	H_{Ce}
Ni_4 in Ce/Zr-UiO-66 (33.3%)	H_{Ce}-Ni_4
Ni_8 in Ce/Zr-UiO-66 (33.3%)	H_{Ce}-Ni_8
Ni_{12} in Ce/Zr-UiO-66 (33.3%)	H_{Ce}-Ni_{12}
Ni_{16} in Ce/Zr-UiO-66 (33.3%)	H_{Ce}-Ni_{16}
Ti/Zr-UiO-66 (16.6%)	L_{Ti}
Ni_4 in Ti/Zr-UiO-66 (16.6%)	L_{Ti}-Ni_4
Ni_8 in Ti/Zr-UiO-66 (16.6%)	L_{Ti}-Ni_8
Ni_{12} in Ti/Zr-UiO-66 (16.6%)	L_{Ti}-Ni_{12}
Ni_{16} in Ti/Zr-UiO-66 (16.6%)	L_{Ti}-Ni_{16}
Ti/Zr-UiO-66 (33.3%)	H_{Ti}
Ni_4 in Ti/Zr-UiO-66 (33.3%)	H_{Ti}-Ni_4
Ni_8 in Ti/Zr-UiO-66 (33.3%)	H_{Ti}-Ni_8
Ni_{12} in Ti/Zr-UiO-66 (33.3%)	H_{Ti}-Ni_{12}
Ni_{16} in Ti/Zr-UiO-66 (33.3%)	H_{Ti}-Ni_{16}
Planar Ni_4 in octahedral void of UiO-66 (Zr)	oct-UiO-66
Planar Ni_4 in octahedral void of Ce/Zr-UiO-66 (16.6%)	oct-L_{Ce}-Ni_4
Another Ni_4 configuration in tetrahedral void	tet-L_{Ce}-Ni_4
Ni_8 in octahedral void	oct-L_{Ce}- Ni_8
Ni_8 in other tetrahedral void	tet-L_{Ce}-Ni_8

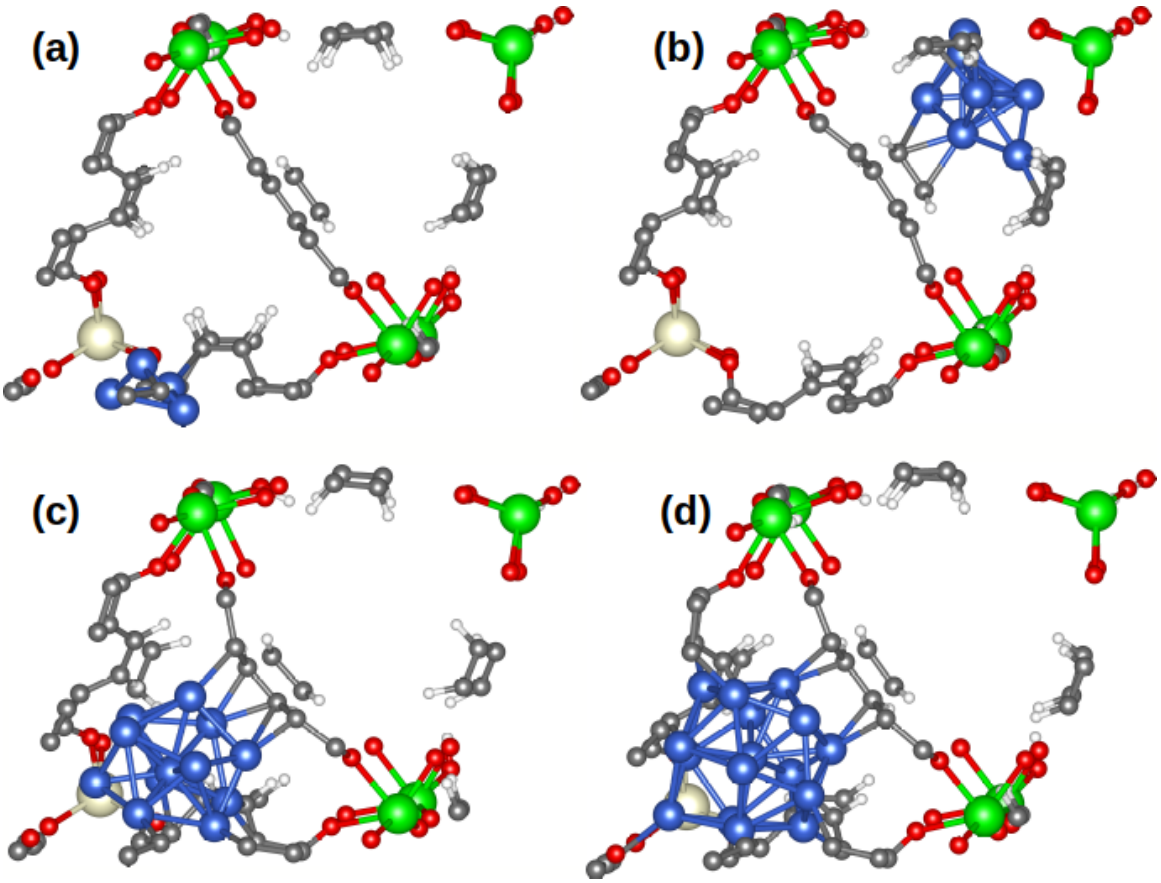

Figure S1: Stable configurations of Ni_x (x=4-16) clusters in the pores of Ce/Zr-UiO-66 (16.6%), (a) L_{Ce}-Ni_4, (b) L_{Ce}-Ni_8, (c) L_{Ce}-Ni_{12} and (d) L_{Ce}-Ni_{16}. Color coding: Cream- Ce, Green- Zr, Grey- C, Red- O, White- H and Blue- Ni.

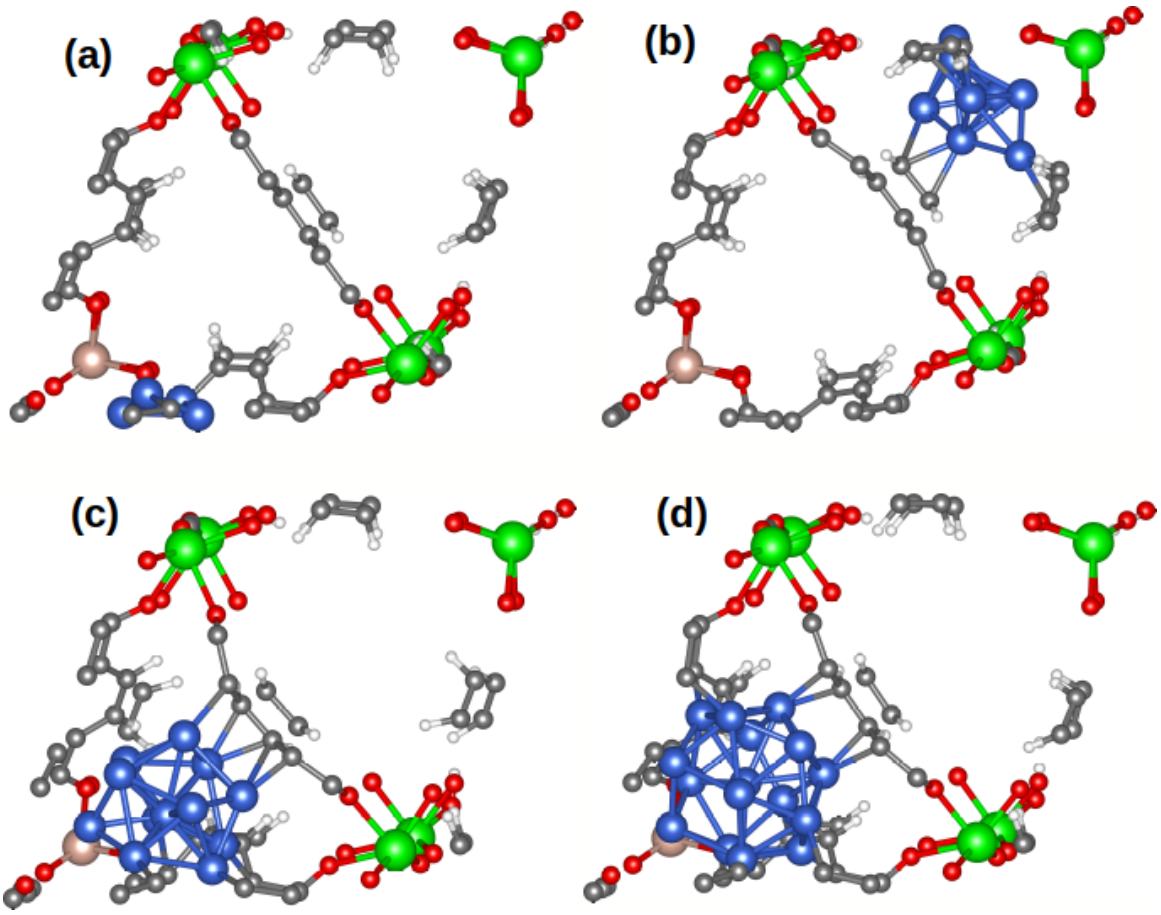

Figure S2: Stable configurations of Ni_x (x=4-16) clusters in the pores of Ti/Zr-UiO-66 (16.6%), (a) L_{Ti}-Ni_4, (b) L_{Ti}-Ni_8, (c) L_{Ti}-Ni_{12} and (d) L_{Ti}-Ni_{16}. Color coding: Pink- Ti, Green- Zr, Grey- C, Red- O, White- H and Blue- Ni.

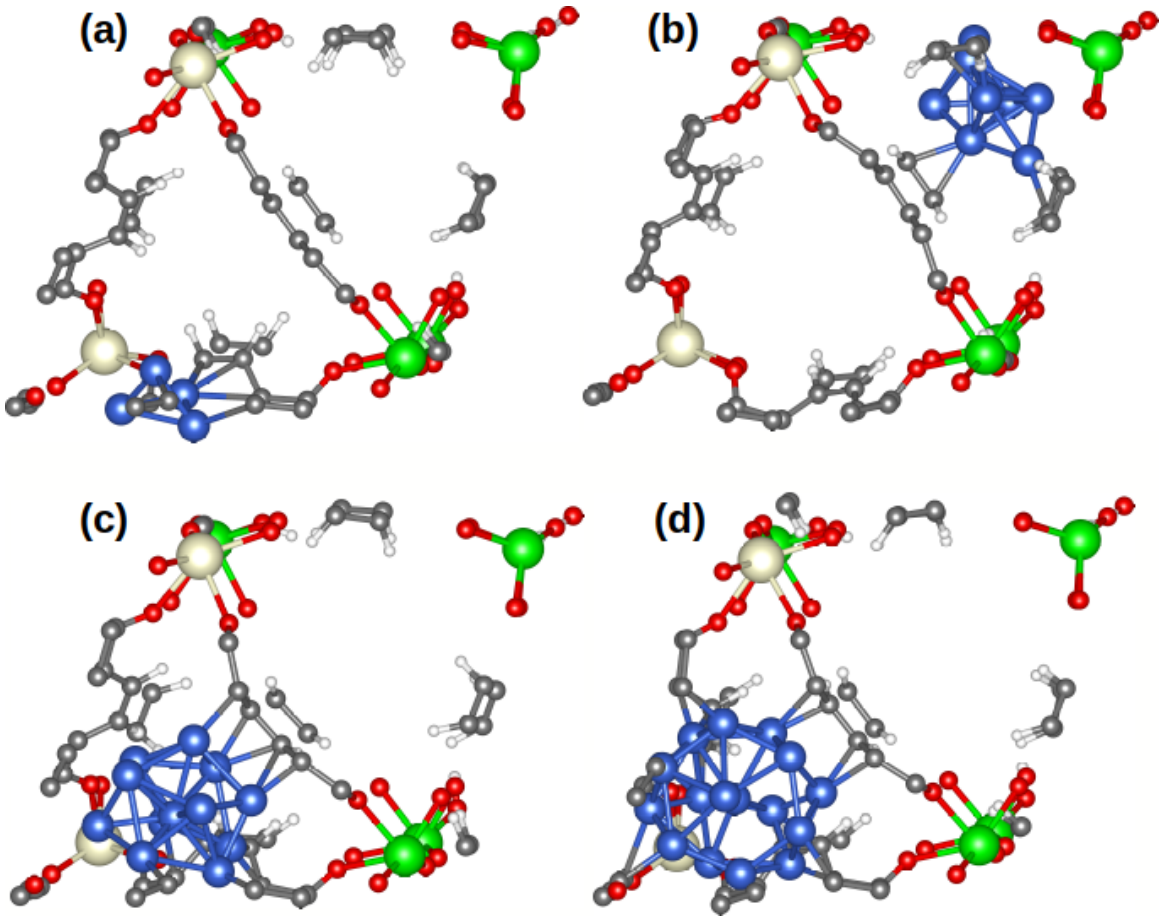

Figure S3: Stable configurations of Ni_x (x=4-16) clusters in the pores of Ce/Zr-UiO-66 (33.3%). (a) H_{Ce}-Ni_4, (b) H_{Ce}-Ni_8, (c) H_{Ce}-Ni_{12} and (d) H_{Ce}-Ni_{16}. Color coding: Cream- Ce, Green- Zr, Grey- C, Red- O, White- H and Blue- Ni.

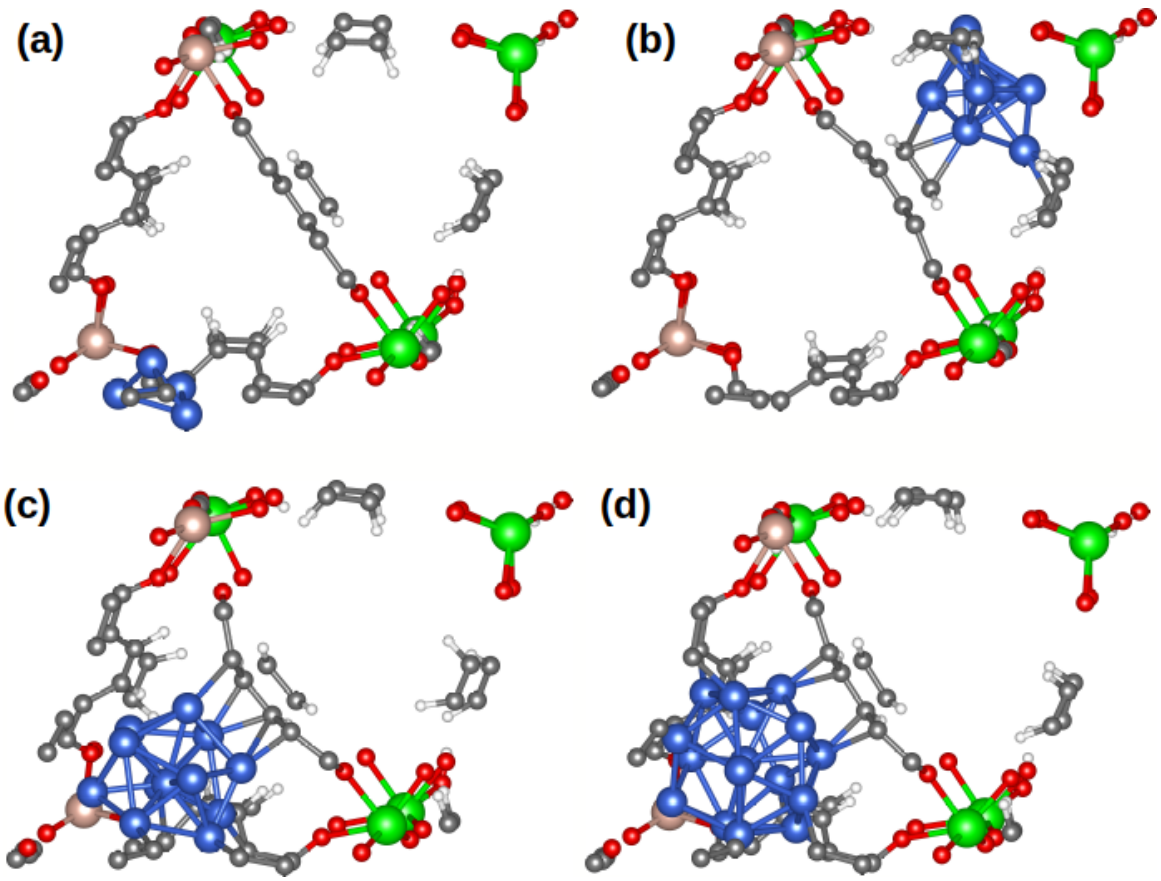

Figure S4: Stable configurations of Ni_x (x=4-16) clusters in the pores of Ti/Zr-UiO-66 (33.3%). (a) H_{Ti}-Ni_4, (b) H_{Ti}-Ni_8, (c) H_{Ti}-Ni_{12} and (d) H_{Ti}-Ni_{16}. Color coding: Pink- Ti, Green- Zr, Grey- C, Red- O, White- H and Blue- Ni.

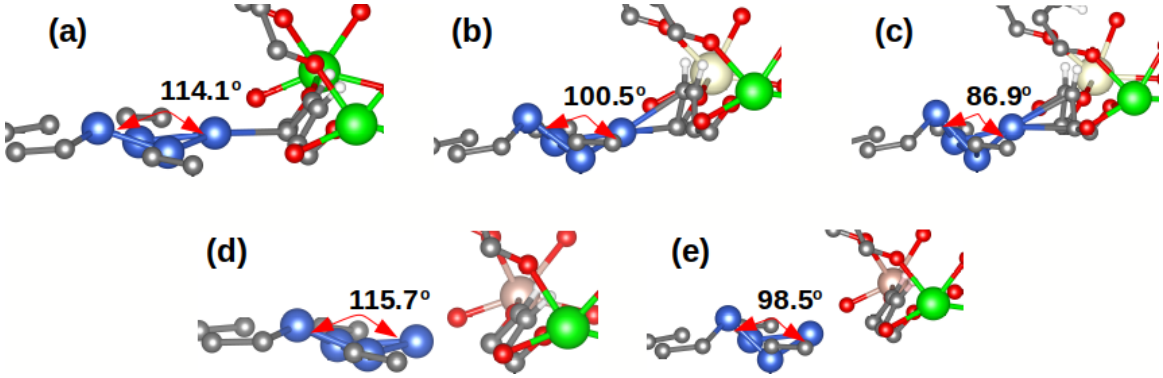

Figure S5: Ni_4 bending shapes in the different models, (a) UiO-66 (Zr) (114.1^o), (b) L_{Ce}-Ni_4 (100.5^o), (c) H_{Ce}-Ni_4 (86.9^o), (d) L_{Ti}-Ni_4 (115.7^o), and (e) H_{Ti}-Ni_4 (98.5^o)

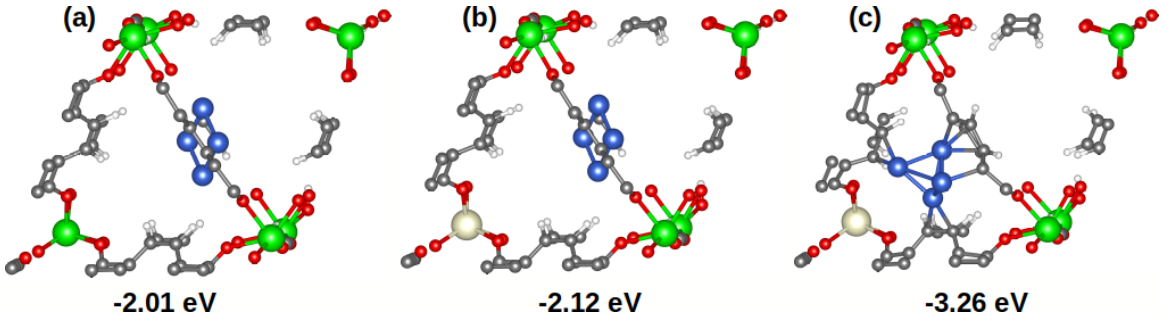

Figure S6: Additional configurations of Ni_4 clusters in octahedral and tetrahedral pores of UiO-66 (Zr) and Ce/Zr-UiO-66 (16.6%). (a) oct-UiO-66, (b) oct-L_{Ce}-Ni_4, and (c) tet-L_{Ce}-Ni_4. Octahedral void occupied planar Ni_4 is not interacted with carbons and has lower binding energies of 2.01 eV (a) and 2.12 eV (b) as compared to tetrahedral binding energy in (c) (-3.26 eV). Color coding: Cream- Ce, Green- Zr, Grey- C, Red- O, White- H and Blue- Ni

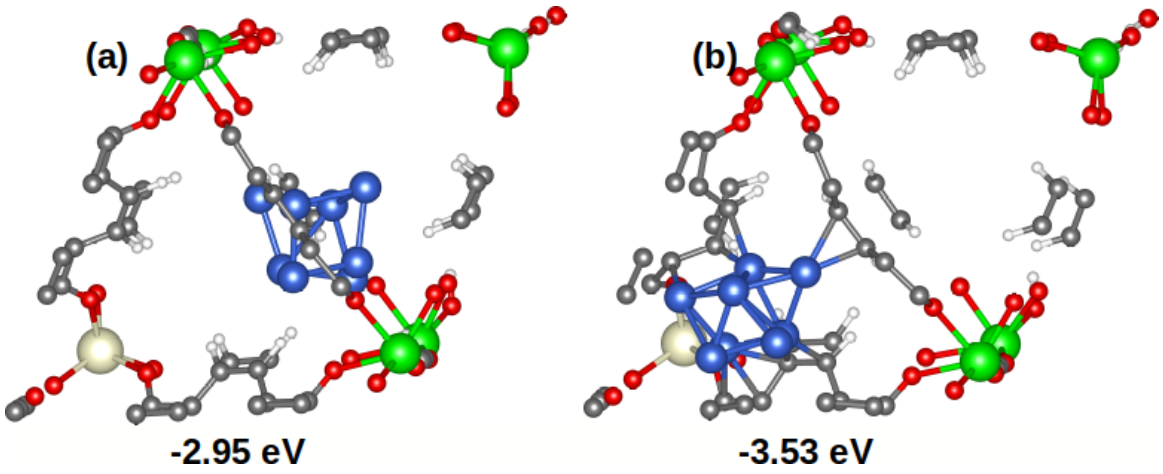

Figure S7: Additional configurations of Ni_8 clusters in octahedral and tetrahedral pores of Ce/Zr-UiO-66 (16.6%). (a) oct-L_{Ce}- Ni_8, and (b) tet-L_{Ce}-Ni_8. The shape of Ni_8 configuration in tetrahedral void changed as compared to octahedral void. Similar to Ni_4, the binding energy of Ni_8 cluster in tetrahedral pore results into higher value of -3.53 eV (b) as compared to octahedral pore (-2.95 eV (a)). Color coding: Cream- Ce, Green- Zr, Grey- C, Red- O, White- H and Blue- Ni

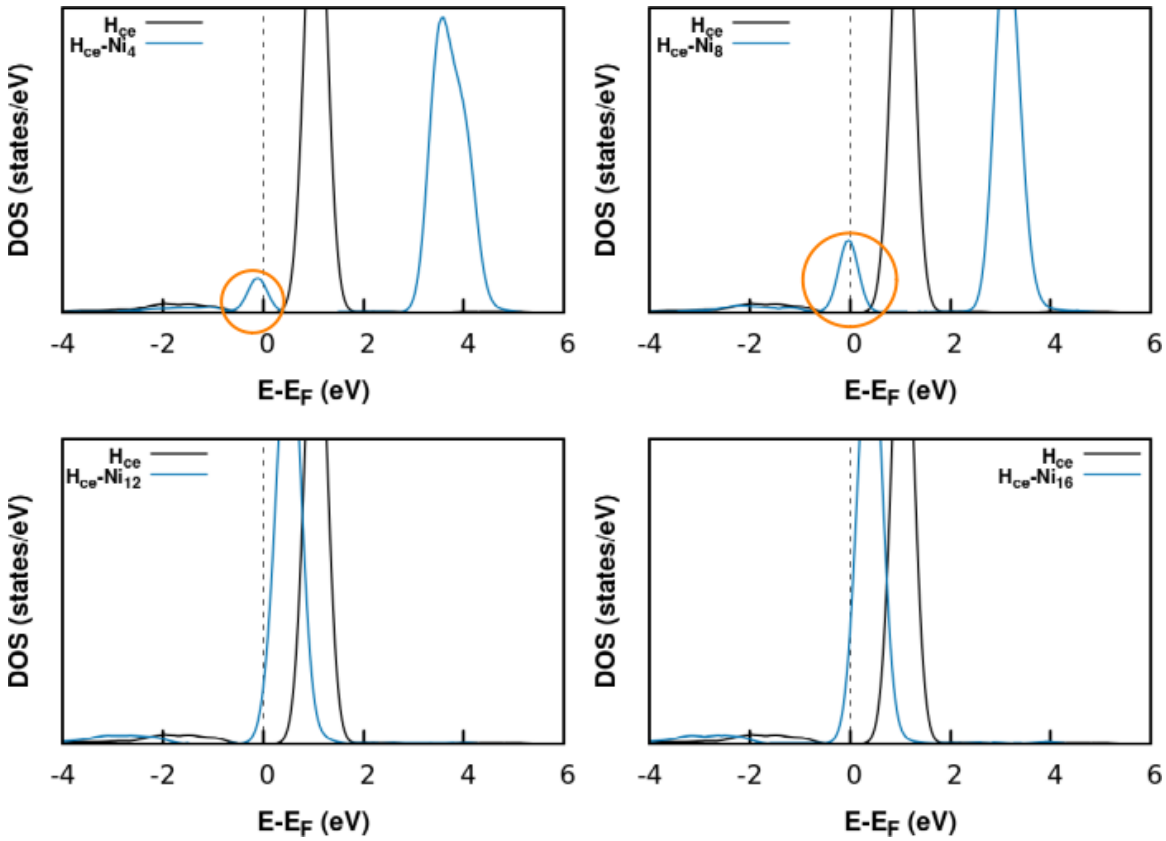

Figure S8: Projected density of states (PDOS) of Ce (4f) before and after impregnation of Ni_x (x=4-16) cluster in Ce/Zr-MOF (33.3%), (a) H_{Ce}-Ni_4, (b) H_{Ce}-Ni_8, (c) H_{Ce}-Ni_{12}, and (d) H_{Ce}-Ni_{16}. Orange circle represent new electronic state of Ce after impregnation of Ni_x cluster

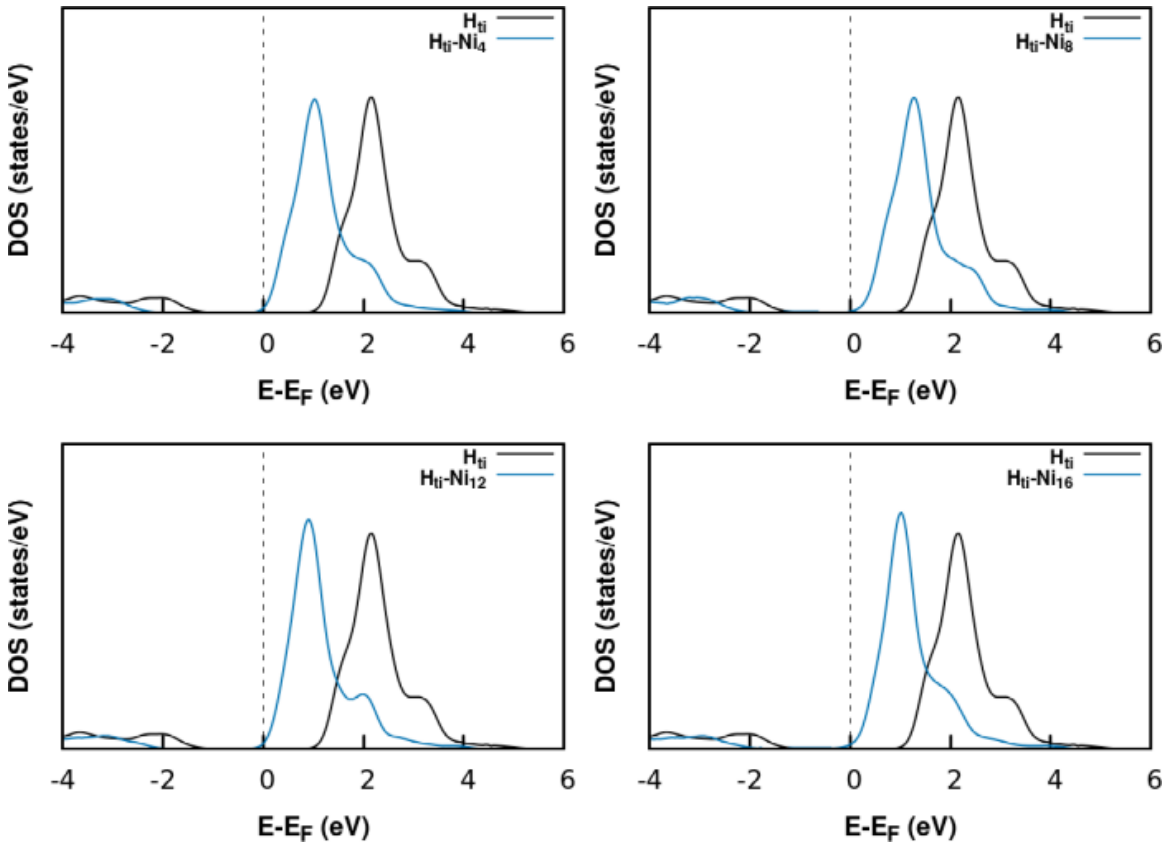

Figure S9: Projected density of states (PDOS) of Ti (3d) before and after impregnation of Ni$_x$ (x=4-16) cluster in Ti/Zr-MOF (33.3%), (a) H$_{Ti}$-Ni$_4$, (b) H$_{Ti}$-Ni$_8$, (c) H$_{Ti}$-Ni$_{12}$, and (d) H$_{Ti}$-Ni$_{16}$

Table S2: Average Löwdin charges of doped metal node (Ce/Ti) in Ce/Zr-UiO-66 (33.3%), and Ti/Zr-UiO-66 (33.3%).

Configuration Name	Avg. charges on Ce/Ti (e)
H_{Ce}	0.45
H_{Ce}-Ni_4	0.55
H_{Ce}-Ni_8	0.45
H_{Ce}-Ni_{12}	0.37
H_{Ce}-Ni_{16}	0.39
H_{Ti}	1.576
H_{Ti}-Ni_4	1.579
H_{Ti}-Ni_8	1.578
H_{Ti}-Ni_{12}	1.585
H_{Ti}-Ni_{16}	1.588